Elsevier Editorial System(tm) for
International Journal of Pharmaceutics
Manuscript Draft

Manuscript Number: IJP-D-17-00438R1

Title: CARVACROL/CLAY HYBRID LOADED INTO IN SITU GELLING FILMS

Article Type: SI: Cyclodextrins

Section/Category:

Keywords: essential oils, palygorskite, carvacrol, cytocompatibility, antimicrobial properties, wound healing

Corresponding Author: Professor Silvia Rossi, Ph.D.

Corresponding Author's Institution: University of Pavia

First Author: Marika Tenci, PhD

Order of Authors: Marika Tenci, PhD; Silvia Rossi, PhD; Aguzzi Carola, PhD; Esperanza Carazo, MD; Giuseppina Sandri, PhD; Maria Cristina Bonferoni, PhD; Pietro Grisoli, PhD; Cesar Viseras, PhD; Carla Marcella Caramella, Pharm.D.; Franca Ferrari, MD

Abstract: The aim of the present work was the development of polymer films loaded with a carvacrol (CVR)/clay hybrid (HYBD) for the delivery of CRV in infected skin ulcer treatment. Different clays were considered: montmorrilonite, halloysite and palygorskite (PHC). CRV incorporation in PHC reduced its volatility. HYBD showed 20% w/w CRV loading capacity and was able to preserve CRV antioxidant properties. HYBD was characterized by improved antimicrobial properties against S. aureus and E. coli and cytocompatibility towards human fibroblasts with respect to pure CRV. Films were prepared by casting an aqueous dispersion containing poly(vinylalcohol) (PVA), poly(vinylpyrrolidone) (PVP), chitosan glutamate (CS), sericin and HYBD. Optimization of film composition was supported by a Design of Experiments (DoE) approach. In a screening phase, a full factorial design (FFD) was used and the following factors were investigated at two levels: PVA (12 - 14% w/w), PVP (2 - 4% w/w) and CS (0.134 - 0.5% w/w) concentrations. For the optimization phase, FFD was expanded to a "central composite design". The response variables considered were: elongation, tensile strength and buffer absorption of films, durability of the gels formed after film hydration. Upon hydration, the optimized film formed a viscoelastic gel able to protect the lesion area and to modulate CRV release.

Dear Sirs,

please find here enclosed the revised manuscript entitled “Carvacrol/clay hybrids loaded into in situ gelling films” by M. Tenci, S. Rossi, C. Aguzzi, E. Carazo, G. Sandri, M.C. Bonferoni, P. Grisoli, C. Viseras, C.M. Caramella, F. Ferrari, submitted for publication on International Journal of Pharmaceutical (Special issue dedicated to Prof. D. Duchene).

The novelty of the present work lies in the development of carvacrol/palygorskite hybrid to be used in the treatment of skin ulcers. CRV loading into hybrid protects CRV from evaporation and allows a CRV controlled release. This reduces carvacrol cytotoxicity towards human fibroblasts, increases its antimicrobial activity and maintains its antioxidant properties. Films characterized by optimal mechanical and hydration properties able to load hybrid and to form a viscoelastic gel upon contact with wound exudate is developed.

Thank you for the attention

Best regards

Silvia Rossi

Associate Professor
Department of Drug Sciences
University of Pavia
Viale Taramelli, 12
27100 Pavia
Phone +39 3334987486
Fax +39 0382 422975
e-mail: silvia.rossi@unipv.it

*Graphical Abstract (for review)

No CRV evaporation

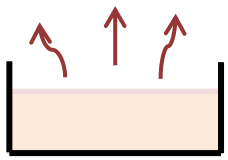

CRV controlled release

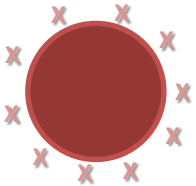

Protection of human fibroblasts against CRV cytotoxic effect and oxidative damages

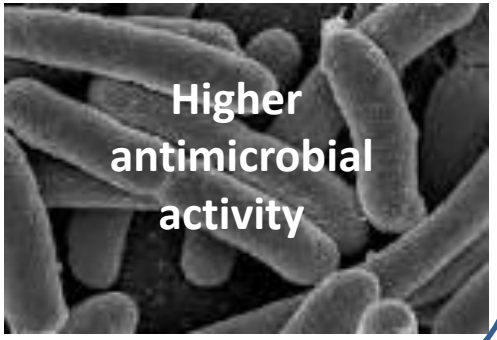

CVR/CLAY HYBRID

LOADED INTO

IN SITU GELLING FILM

PVA - PVP - CS - SER - GLY

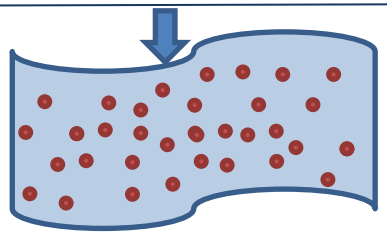

wound

exudate

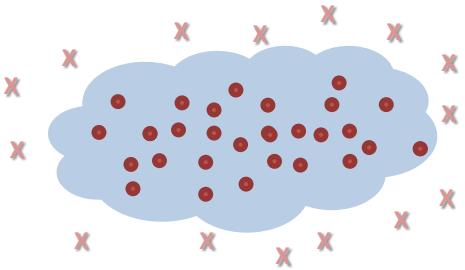

VISCOELASTIC GEL

mechanical protection of the lesion area, improvement of fibroblast proliferation (CS, SER)

CRV: carvacrol; PVA: polyvinylalcohol; PVP: polyvinylpyrrolidone; CS: chitosan; SER: sericin; GLY: glycerol

Carvacrol/clay hybrids loaded into *in situ* gelling films

Tenci M[1]., Rossi S[1, 2]., Aguzzi C[3]., Carazo, E[3]., Sandri G[1, 2]., Bonferoni M.C[1, 2]., Grisoli P[1]., Viseras C[3,4]., Caramella C.M[1]., Ferrari F[1, 2].

[1]Department of Drug Sciences, University of Pavia, v.le Taramelli 12, 27100 Pavia, Italy

[2]CHT, Centre for Health Technology, University of Pavia, 27100 Pavia, Italy

[3]Department of Pharmacy and Pharmaceutical Technology, University of Granada, Campus of Cartuja, Granada, 18071 s/n, Spain

[4]Andalusian Institute of Earth Sciences, CSIC-University of Granada, Avenida de las Palmeras, Armilla, Granada, Spain.

Corresponding author:
Silvia Rossi, Department of Drug Sciences, University of Pavia, Viale Taramelli 12, 27100 Pavia
Tel.: +39 0382 987357; fax: +39 0382 422975.
E-mail address: silvia.rossi@unipv.it

ABSTRACT

The aim of the present work was the development of polymer films loaded with a carvacrol (CVR)/clay hybrid (HYBD) for the delivery of CRV in infected skin ulcer treatment. Different clays were considered: montmorrilonite, halloysite and palygorskite (PHC). CRV incorporation in PHC reduced its volatility. HYBD showed 20% w/w CRV loading capacity and was able to preserve CRV antioxidant properties. HYBD was characterized by improved antimicrobial properties against *S. aureus* and *E. coli* and cytocompatibility towards human fibroblasts with respect to pure CRV.

Films were prepared by casting an aqueous dispersion containing poly(vinylalcohol) (PVA), poly(vinylpyrrolidone) (PVP), chitosan glutamate (CS), sericin and HYBD. Optimization of film composition was supported by a Design of Experiments (DoE) approach. In a screening phase, a full factorial design (FFD) was used and the following factors were investigated at two levels: PVA (12 - 14% w/w), PVP (2 - 4% w/w) and CS (0.134 - 0.5% w/w) concentrations. For the optimization phase, FFD was expanded to a "central composite design". The response variables considered were: elongation, tensile strength and buffer absorption of films, durability of the gels formed after film hydration. Upon hydration, the optimized film formed a viscoelastic gel able to protect the lesion area and to modulate CRV release.

Key-words: essential oils, palygorskite, carvacrol, cytocompatibility, antimicrobial properties, wound healing

1 INTRODUCTION

Chronic wounds, such as diabetic foot ulcers, pressure ulcers and venous leg ulcers represent a worldwide health problem (Boateng et al., 2008; Boateng and Catanzano, 2015). Advanced therapeutic dressings, designed to take an active role in the wound healing process, represent an interesting approach in the treatment of chronic wounds. Their biological properties are related not only to the bioactive agents loaded into dressing, but also to the presence of biomaterials able to improve tissue repair (Boateng and Catanzano, 2015). Among these biomaterials, chitosan, a linear polysaccharide obtained by chitin deacetylation, has been recognized as a biopolymer able to promote tissue repair and to avoid the onset of infections (Muzzarelli, 2009, Rossi et al., 2010; Rossi et al., 2013; Mori et al., 2016; Tenci et al., 2016).

The association of synthetic and natural polymers in composite dressings has been recognized useful to control drug delivery in the wound site (Boateng et al., 2008). Among synthetic polymers, poly(vinylalcohol) (PVA) and poly(vinylpyrrolidone) (PVP) have been largely employed for biomedical applications, such as controlled release systems and tissue engineering (Li et al., 2010; Vicentini et al., 2010).

Carvacrol (CRV), a monoterpene phenolic compound, is the major component (up to 80%) of oregano essential oil (*Origanum vulgare)* (Burt, 2004). It possesses antioxidant, antifungal and antimicrobial properties (Ben Arfa et al., 2006; Safaei-Ghomi et al., 2009; Tunç et al., 2011). Different strategies were proposed to reduce evaporation of EOs. One of these provides the inclusion of EOs in montmorrilonite (MMT) and halloysite (HAL). Recently, some authors proposed the use of such clays as packaging materials and demonstrated their capability to enhance the thermal stability and to preserve the antimicrobial properties of EOs (Efrati et al., 2014; Shemesh et al., 2015). Gorrasi et al. (2015) proved that packaging hybrid/polymer films were able to control EOs release.

So far, to the best of our knowledge, no papers have been published on the use of EO/clay hybrids loaded into films for cutaneous application. Clays generally employed in the pharmaceutical and cosmetic fields belong to smectites, kaolin and fibrous clay groups (López-Galindo et al., 2007; Viseras et al., 2008, 2010; Sánchez-Espejo et al., 2014).

Given these premises, the aim of the present work was the preparation of CVR/clay hybrids to be loaded into gelling viscoelastic films for the treatment of infected skin lesions. Hybrids should prevent CVR evaporation and maintain its antioxidant and antimicrobial properties. Three different commercial clays have been considered: MMT, HAL and palygorskite (PHC).

In a first phase of the research, CVR and CVR/clay hybrids were prepared by using two different approaches: adsorption in saturated atmosphere and shear mixing. Hybrids were subjected to

thermal analysis in order to study the effect of clay type and of preparation method on CRV volatility. On the basis of the results obtained, clay and preparation method which allowed the highest CRV loading were chosen for the continuation of the research. The chosen CRV/clay hybrid (HYBD) was investigated *in vitro* for cell viability and antioxidant activity on human fibroblasts and for antimicrobial properties on *S. aureus* and *E. coli*, in comparison with pure CRV.
A second phase of the research was devoted to the preparation and optimization of films to be used as vehicle for HYBD. Films should be characterized by suitable mechanical properties (high flexibility and resistance to rupture) and by the capability to absorb wound exudate forming a viscoelastic persistent gel, able to protect the lesion area without impairing CRV release.
Films were composed by poly(vinylalcohol) (PVA), poly(vinylpirrolidone) (PVP), chitosan glutamate (CS), sericin (SER) and glycerol. PVA was used for its excellent film-forming capacity (Guo et al., 2011; Comolli et al., 2012). PVP was combined with PVA as a controller of mechanical property because this polymer had good aqueous solubility and extremely low cytotoxicity (Contardi et al., 2017; Sreedharan and Sujith , 2015; Seabra and De Oliveira, 2004; Singh and Pal, 2011). CS was chosen for its capability to enhance wound healing (Rossi et al., 2015). Sericin (SER) was added to improve HYBD antioxidant properties (Mori et al., 2016), while glycerol was used as plasticizing agent. To obtain films of optimized composition, a DoE approach was employed. The experimental design provided a screening and an optimization phase. In the screening phase a two full factorial design was used not only to investigate the effect of each factor (PVA, PVP and CS concentrations) on the response variables considered (flexibility, mechanical strength, hydration capability of films and gel durability), but also to individuate the main influencing factors. To find the optimal formulation, the screening design was expanded to a central composite design (CDD) (Dejagher and Vander Heyden, 2011). The experimental results characterizing the optimized formulation were compared to those predicted by the model in order to confirm its predictive power. Moreover, film of optimized composition was subjected to rheological (viscoelastic) characterization upon hydration in a medium mimicking wound exudate and to *in vitro* CRV release measures.

2 MATERIALS AND METHODS

2.1 Materials

The following materials were used: antibiotic/antimycotic solution (100×), containing 10,000 units/ml penicillin, 10 mg/ml streptomycin and 25 µg/ml amphotericin B (Sigma Aldrich, Milan, I); carvacrol (natural, 99%, FG; CRV) (Sigma Aldrich, Milan, I); chitosan low MW (CS) (DD: 80%) (Sigma Aldrich, Milan, I); dimethyl sulfoxide (DMSO) (Sigma Aldrich, Milan, I); Dulbecco's

Modified Eagles Medium (DMEM) (Lonza, BioWhittaker, Walkersville, MD, USA); Dulbecco's Phosphate Buffer Solution (Sigma Aldrich, Milan, I); glutamic acid (Sigma Aldrich, Milan, I); glycerol (Carlo Erba, Milan I); Hank's balanced salt solution (HBSS) (Sigma Aldrich, Milan, I); inactivated foetal calf serum (Biowest, Nuaillé, F); hydrogen peroxide (Carlo Erba, Milan, I); MTT (3-(4,5-dimethylthiazol-2-yl)-2,5-diphenyltetrazolium bromide) (Sigma Aldrich, Milan, I); $NaH_2PO_4 \cdot H_2O$ (Carlo Erba, Milan I); $Na_2HPO_4 \cdot H_2O$ (Carlo Erba, Milan, I); NaCl (Carlo Erba, Milan, I); n-hexane (Carlo Erba, Milan I); Pharmasorb© colloidal (Palygorskite, PHC) (BASF Aktiengesellschaft, Ludwigshafen, G); poly(vinylalcohol) (PVA) (Sigma Aldrich, Milan, I); poly(vinylpyrrolidone) K90 (PVP) (BASF Aktiengesellschaft, Ludwigshafen, G); trypan blue solution (Biological Industries, Beit-Haemek, IL); trypsin–EDTA solution (Sigma Aldrich, Milan, I); Veegum© HS (montmorillonite, MMT) (Vanderbilt Minerals, LLC, Norwalk, USA); Halloysite (HAL) (Sigma Aldrich, Madrid, S).

2.2 Preparation of CVR/clay hybrids

Three different clays, halloysite (HAL), montmorrilonite (MMT) and a commercial palygorskite (PHC) were considered. CVR/clay hybrids were prepared according to two different methods: adsorption in saturation conditions and shear mixing.

The first method provided to create an ambient saturated with CVR. To this aim, a beaker containing 10 ml of CVR was put in the middle of an hermetically sealed glass chamber (489 cm^3 volume). 50 mg of each clay was layered on a watch glass inside of the chamber. The chamber was thermostatated at a constant temperature (20, 40, 60, 80 and 120°C) for a fixed time period (2 or 5 days).

Shear mixing technique provided to disperse the clay in CVR (2:1 w/w ratio) by ultra-sonication at room temperature for 1 h (Shemesh et al., 2015). CVR not adsorbed onto clay was removed by centrifugation (4218 centrifuge, ALC International s.r.l., Milan, I) at 1000 g for 15 min and by evaporation in oven (Vismara Laselelettronics s.r.l., Lodi, I) for 24 h at 80°C.

To assess CRV loading, CVR/clay hybrids were subjected to thermogravimetric analysis (TGA). Pure CVR and clays were used as references. TGA analysis was carried out by a Shimadzu mod. TGA-50H apparatus, in the temperature range 36–950°C at a heating rate of 10°C/min. The results were expressed as % mass loss as a function of temperature. From the comparison of TGA profiles of hybrids with those of pure CVR and clays, % CRV loading into hybrids was calculated (% LC) (see Eq. 1).

$$\% \text{ LC} = \frac{\text{CVR loaded (mg)}}{\text{hybrid (mg)}} \times 100 \qquad \textbf{Eq. (1)}$$

TGA analysis was also used to assess HYBD stability upon storage for 1 month at 20°C in a desiccator.

To confirm the data obtained from TGA analysis, the amount of CRV loaded into HYBD was assessed by an extraction method. In particular, 2 mg of HYBD was weighted and added to 10 ml n-hexane (Tunç and Duman, 2011). The dispersion was maintained under stirring overnight, centrifuged at 3000 rpm for 20 min and then filtered (cellulose acetate, 0.45 µm; Sartorius, Muggiò, I). The supernatant was recovered and analyzed for CRV content by means of a UV-vis spectrophotometer (Perkin Elmer, Lambda 25) at wavelengths ranging from 200 to 500 nm. A calibration curve was obtained using CRV hexane solutions having the following concentrations: 50, 25, 20, 10 and 5 µg/ml.

2.3 *In vitro* cytocompatibility assessment of CRV and HYBD

NHDF (normal human dermal fibroblasts from foreskin) (Promocell GmbH, Heidelberg, G) 6^{th} to 16^{th} passage were used.

Cells were cultured in a polystyrene flask (Greiner bio-one, PBI International, Milan, I) with 13-15 ml of complete culture medium (CM), consisting of Dulbecco's modified Eagles medium with 4.5 g/l glucose and l-glutamine supplemented with 1% (v/v) antibiotic antimycotic solution (100×), stabilized with 10,000 units/ml penicillin, 10 mg/ml streptomycin and 25 µg/ml amphotericin B and 10% (v/v) inactivated fetal calf serum. Cells were maintained in incubator (Shellab® Sheldon® Manufacturing Inc., Oregon, USA) at 37°C under 95% air and 5% CO_2 atmosphere. All the operations required for cell culture were carried out in a vertical laminar air flow hood (Ergosafe Space 2, PBI International, Milan, I). When cells reached 80-90% confluence, trypsinization was effected as described by Tenci et al. (2017). The amount of viable cells in the suspension after trypsinization was determined in a counting chamber (Hycor Biomedical, Garden Grove, California, USA), using 0.5% (w/v) trypan blue solution.

To assess cytocompatibility of CRV and HYBD towards human fibroblasts, cell viability tests were performed to estimate the number of viable cells after a prefixed time-contact with the samples examined.

$3.5 \cdot 10^4$ cell/well (0.35 cm^2 area) were seeded in 96-well plate (Greiner bio-one, VWR International, Milan, I) with culture medium (CM) and let growing to confluence. After medium removal, cells were put in contact for 24 h with 200 µl of CRV aqueous solutions or HYBD aqueous dispersions. In particular, a CRV aqueous solution (1 mg/ml) was diluted in CM; the final concentrations upon dilution were 5, 10, 25 and 50 µg/ml. As for HYBD, the powder was dispersed into CM in order to

obtain final concentrations of CRV equal to 5, 10, 25 and 50 µg/ml. CM was used as positive control. After 24 h contact with samples, cells were washed with 100 µl of HBSS (pH 7.4) and then put in contact for 3 h with a 8 mM MTT (3-(4,5-dimethylthiazol-2-yl)-2,5-diphenyltetrazolium bromide) solution in HBSS (150 µl/well). Finally, 100 µl of dimethylsulfoxide (DMSO) was added to each well, to allow complete dissolution of formazan crystals, obtained from the reduction of MTT dye into cells by dehydrogenase enzyme. After 60 s shaking, the solution absorbance was determined at 570 nm, with a 690 nm reference wavelength, by means of an IMark® Microplate reader (Bio-Rad Laboratories S.r.l., Segrate, Milan, I). Results were expressed as % viability calculated by normalizing the absorbance measured after contact with samples with that measured after contact with pure CM, used as positive control.

2.4 *In vitro* assessment of antioxidant properties of CRV and HYBD

CVR and HYBD antioxidant properties were investigated using fibroblasts as biological substrate. NHDF fibroblasts (Promocell GmbH) from 6^{th} to 16^{th} passage were used. Cells were seeded (3.5 x 10^4 cells/cm^2) overnight into a 96-well plate (Greinerbio-one, PBI International, I) and then put in contact for 6 h with samples (200µl). CRV and HYBD were diluted/ dispersed into complete medium (CM) in order to obtain final concentrations of CRV equal to 5, 10 and 25 µg/ml. Subsequently, 10 µl of 10.5 mM H_2O_2 was added in each well (the final H_2O_2 concentration, upon dilution with 200 µl of CM or sample solution/dispersion, was equal to 1 mM) and incubated for 18h (Mori et al., 2016; Peng et al. 2016). Then, cells were washed with HBSS (pH 7.4) and a MTT test was performed (as described in section 2.3).

2.5 *In vitro* assessment of antimicrobial properties of CRV and HYBD

To evaluate the antimicrobial properties of CRV and HYBD, the following reference bacterial strains were used: *Staphylococcus aureus* ATCC 6538 and *Escherichia coli* ATCC 10536. Before testing, bacteria were grown overnight in Tryptone Soya Broth (Oxoid, Basingstoke, UK) at 37°C. The cultures were centrifuged at 224g for 20 min to separate microorganisms from culture broth and then washed with purified water. Washed cells were re-suspended in Dulbecco's PBS and optical density (OD) was adjusted to 0.1, corresponding approximately to 1×10^8 colony forming units (CFU) /ml at 650 nm wavelength.

The antimicrobial activity of CRV and HYBD was determined with the macrodilution broth method, according to Clinical and Laboratory Standards Institute guidelines (2009), with some modifications reported in this paragraph. The desired concentration of CRV was achieved through

the addition in 15 mm × 100 mm test tubes of an appropriate CRV volume to 1 ml of double-concentrate Iso-Sensitest broth (ISB, Oxoid). Bacterial suspensions were added to the test tubes. The minimum inhibitory concentration (MIC) was evaluated after 24 h incubation at 37°C as the lowest concentration that completely inhibited the formation of visible microbial growth. Control test tubes containing microorganisms in culture without CRV were used. The same experiment was performed suspending an appropriate quantity of HYBD in 1 ml of double-concentrated Iso-Sensitest broth (ISB, Oxoid). Test tubes containing each microorganism in culture added with unloaded clay were used as controls. MIC was detected after 24 h incubation at 37°C.
Minimum bactericidal concentration (MBC) was evaluated by inoculating aliquots of culture medium in which the inhibition of bacterial proliferation was observed. MBC was the lowest concentration capable of killing the microbial cells (Clinical and Laboratory Standards Institute, 1999). MBC was detected after 24 h incubation at 37°C . Bacteria-free broth was included as control.

2.6 DoE assisted approach for film formulation

2.6.1 Screening of independent variables

A screening design was used to determine which factors and which of their interactions significantly affect the response variables. Such factors would have been subsequently considered in the optimization phase. Full or fractional two-level factorial designs could have been employed for this purpose (Dejaegher and Vander Heyden, 2011).
In the present work a "2^3 full factorial design" (FFD) was chosen. Three factors, corresponding to the three polymers employed for film formulation, PVA, PVP and CS, were investigated at two different concentrations (levels). The polymer concentrations considered were: 12%, 14% w/w for PVA (x_1), 2%, 4% for PVP (x_2) and 0.134%, 0.5% w/w for CS (x_3). Eight film formulations, corresponding to the different experimental points, were prepared. In Table 1 (points 1-8) polymer concentrations employed for film preparation are reported: for each polymer the upper level is indicated as +1 and the lower one as -1. The response variables considered were: % elongation (%E), tensile strength (TS), hydration properties (buffer amount absorbed per unit weight) and gel durability. The experiments were performed in random sequence. Design generation and statistical analysis were carried out using a statistical software package (Statgraphics 5.0 Statistical Graphics Co., Rockvillle, MD, USA).

2.6.2 Optimization design

For the optimization of film formulation, a response surface design, in particular a randomized "central composite design" (CDD), was used.

Response surface designs are divided into 2 categories, symmetrical and asymmetrical designs; in particular CDD is a symmetrical response surface design and covers a symmetrical experimental domain (Dejaegher and Vander Heyden, 2011). In this type of design the dependent variables are modelled as function of the independent parameters.

CDD consists of three parts: (1) a full factorial design (2^f experiments), (2) an additional design, a star design ($2*f$ experiments), and (3) a central point. N experiments ($N=2^f+(2*f)+1$) are required to examine the most important factors (f) identified by the preliminary screening design.

In CDD, the experimental points of the full factorial design correspond to the levels -1 and +1, those of the star design at the levels 0, $-\alpha$ and $+\alpha$ ($\alpha \geq 1$), and the central point at the level 0.

Depending on α value, two different CCDs exist: a face-centred CCD ($\alpha=1$), a simplified CDD, in which three levels for each factor are considered, and a circumscribed CCD ($\alpha>1$), examining the factors at five levels (Dejagher and Vander Heyden, 2011).

For our purpose a CDD with $\alpha>1$, examining five levels for each factor, was considered and seven additional dressing formulations were investigated with respect to FFD (Table 1 (points 9-15)).

The factors and the response variables considered in CDD were the same of the screening phase.

The experiments were performed in random sequence. Design generation and statistical analysis were carried out using a statistical software package (Statgraphics 5.0 Statistical Graphics Co., Rockvillle, MD, USA).

In the optimization phase, experimental data obtained for each response variable of the experimental design were fitted to a multiple regression model, described below (Eq. (2)):

$$y = \beta_0 + \sum_{i=1}^{f} \beta_i x_i + \sum_{1 \leq i < f}^{f} \beta_{ij} x_i x_j + \sum_{i=1}^{f} \beta_{ii} x_i^2 \qquad \textbf{Eq. (2)}$$

where y is the response, β_0 the intercept, β_i the main coefficients, β_{ij} the two-factor interaction coefficients, and β_{ii} the quadratic coefficients (Dejaegher and Vander Heyden, 2011; Ćurić A. et al., 2013).

Such model was used to predict the value of each response variable, related to any combination of factors within the experimental region, by means of a software package (Statgraphics 5.0, Statistical Graphics, Rocknille, MD). It was also possible to compare the predicted values with the

experimental data by using the Analysis of Variance (ANOVA) (Dejagher and Vander Heyden, 2009, 2011).

2.6.3 Film preparation

HYBD at 2.6% w/w concentration was dispersed into a sericin (Ser) (1.6% w/w)/glycerol (gly) (20% w/w) aqueous solution. Ser was used to strengthen CRV antioxidant properties (Mori et al., 2016), whereas gly acted as plasticizer (Rossi et al., 2013). Such a dispersion was diluted 1:1 w/w with a polymeric aqueous solution, containing PVA, PVP and CS.

The final polymer concentrations corresponded to the different points of the experimental design. After overnight stirring, 6.7 g of the diluted dispersion was layered on teflon plates (5.5 cm × 5.5 cm area) and dried for 24 h at 50°C in oven (Vismara Laser Elettronics s.r.l., Lodi, I). After drying, films were recovered and stored in a desiccator until characterization. Dried films were characterized for CRV loading, mechanical properties, buffer absorption properties and for the durability of gel formed upon hydration in a medium mimicking wound exudate.

2.6.4 CRV loading into films

In order to quantify the amount of CRV loaded into films, 100 mg of each film was dissolved in 1 ml of distilled water. Subsequently, 10.0 ml of n-hexane was added. To allow the complete CRV extraction the aqueous-organic mixture was maintained under stirring overnight (Campos-Requena, 2015). The mixture was centrifuged at 1000 g for 20 min to separate the organic from the aqueous phase. Finally, the organic phase recovered was filtered through a cellulose acetate membrane (cellulose acetate, 0.22 μm; Sartorius, Muggiò, I) and analyzed with a UV-vis spectrophotometer (Perkin Elmer, Lambda 25) as described in the paragraph 2.2.

2.6.5 Assessment of film mechanical properties

Mechanical properties were measured using a TA-XT plus Texture Analyzer (ENCO, Spinea, Venice, I) equipped with a 5 kg load cell. Before testing, dried films were cut 40 mm x 20 mm and the strips obtained were clamped between tensile grips A/TG probe, setting an initial distance between the grips of 20 mm. Then, the upper grip was raised at a constant speed of 5 mm/s up to a distance equal to 20 mm, corresponding to 100% elongation. Films were visually inspected in order to observe the occurrence of a physical damage (break) during the test. % elongation corresponding to film break was recorded together with the related tensile strength applied (TS, N/mm^2). In absence of film damage, tensile strength value corresponding to 100% elongation was recorded.

TS is an index of film strength, while %E indicates film flexibility, that is the capability of the film to deform without breaking when subjected to increasing strengths (El-Malah and Nazzal, 2008). Percent elongation was calculated as follow (Eq. (3)):

$$\% E = \frac{\text{final lenght - initial lenght}}{\text{initial lenght}} \times 100 \qquad \textbf{Eq. (3)}$$

2.6.6 Assessment of film hydration properties and gel durability

Films were subjected to hydration measurements at 32°C by means of Franz diffusion cells (PermeGear, Bethlehem (PA)). A circular film, having a diameter of 20 mm and weight of 200 ± 10 mg, was layered on a pre-hydrated dialysis membrane (Mires Emanuele, MWCO 12-14000 Da; ø 36/32″ - 28.6 mm), used to separate the donor and the receptor chambers of the Franz cell. The receptor chamber was filled with pH 7.4 buffer (phosphate buffered saline (PBS); $NaH_2PO_4 \cdot H_2O$ 0.036% w/w, Na_2HPO_4 H_2O 0.137% w/w, NaCl 0.850% w/w), chosen to mimic wound exudate. At prefixed times (4 and 8 h), films were weighted (Tenci et al., 2017).

The PBS amount taken up by the film was normalized for dry film weight (gPBS/g) to obtain the amount of PBS uptaken/unit film weigth (gPBS/g).

The gel durability was also calculated as the amount of gel formed after 8 h of hydration; it is an index of the dressing resistance against erosion/dissolution process, upon contact with wound exudate.

2.7 Characterization of optimized film formulation

Films of optimized composition (opFILM), chosen on the basis of the results obtained by the CDD design, were prepared by casting (as described in section 2.7.1) and subjected to the same characterization previously effected on the formulations of the full and central composite designs (sections 2.7.2 and 2.7.4). The experimental results obtained for opFILM were compared with those provided by the model, in order to confirm its predictive power. Moreover, opFILM was characterized for CRV loading capacity, rheological and CRV release properties as hereafter described.

2.7.1 Assessment of rheological properties of opFILM after hydration

After 4 h hydration (see paragraph 2.7.4), opFILM was subjected to dynamic viscoelastic (stress sweep and oscillation) tests by means of a rotational rheometer (Rheostress 600, Haake, I), equipped with a cone/plate combination (C20/1: Ø 20 mm; angle=1°) measuring system.

Stress sweep measurements provide to apply increasing shear stress values (ranging from 0.1 up to 50 Pa) at a constant frequency (0.1 Hz) and to measure the viscoelastic response of the sample, expressed as storage modulus (G′), in order to determine the linear viscoelastic region of the sample. Oscillation measurements require to apply a fixed stress chosen in the linear viscoelastic region, previously determined, at increasing frequency values (ranging from 0.1 to 10 Hz) and to measure the viscoelastic response of the sample, expressed as the ratio between loss (G'') and storage (G′) moduli (loss tangent, tan delta).

2.7.2 Assessment of *in vitro* CRV release from opFILM and HYBD

CRV release from opFILM and HYBD was evaluated at 32°C by means of Franz diffusion cells (Permeager, Bethlehem, PA, USA) having a 20 mm diameter orifice (3.14 cm^2). Dried films having a diameter of 10 mm and weighting 100 ± 5 mg were examined. For HYBD, 10.0 ± 0.5 mg of powder was layered on a filter membrane (cellulose acetate, 0.22 μm; Sartorius, Muggiò, I), separating the donor and the receptor chambers of the Franz cell (Mori et al., 2014). The receptor chamber was filled with pH 7.4 PBS. At fixed time periods (4, 8, 24 and 48 h), 1 ml of medium was collected and analyzed at 273 nm.

2.8 Statistical analysis

Whenever possible, experimental values of the various types of measures were subjected to statistical analysis. In particular, Anova one way, multiple range test (MRT) was used (Statgraphics 5.0, Statistical Graphics Corporation, Rockvillle, MD, USA).

3 RESULTS AND DISCUSSION

3.1 Choice of clay type and hybrid preparation method

Figure 1A reports % CRV loading capacity (%LC) of the three different CVR/clay hybrids prepared by adsorption in saturated atmosphere, after 48h storage at different temperatures. For all the three clays, an increase in % LC on increasing temperature was observed. HAL was able to adsorb CVR at temperature higher than 40°C. Among the three clays considered, PHC was characterized by the highest % LC values. This result can be explained by the higher surface available for adsorption of PHC, being a fibrous clay. The highest %LC value was observed at 120°C.

In Figure 1B %LC values of the three different CRV/clay hybrids prepared by shear mixing are reported. Also for this preparation technique, %LC was affected by clay structure: the highest value was observed for the fibrous PHC, followed, in decreasing order, by the tubular HAL and by the lamellar MMT. CVR/PHC hybrid (HYBD) prepared by shear mixing was characterized by % LC

equal to 20% (w/w), greater than that determined after adsorption in saturated atmosphere technique (14% w/w). The comparison of the results obtained for the various clays with the two different techniques addressed the choice on PHC and shear mixing technique

As an example, in Figure 2A TGA profiles of HYBD was compared with those of pure CRV and PHC. CRV shows a clear weight loss, due to CRV evaporation, starting at 36°C and concluded at 191°C. PHC appears as a thermostable clay, characterized by a weight loss step (150°C), corresponding to evaporation of superficial humidity (7.6% w/w), with a solid residue at 950°C equal to approximately 83%. In the TGA profile of HYBD three different steps can be distinguished. The first one (80-286°C) was associated to a 17% weight loss, attributable to a 9.5% w/w CRV loss, taking into account a 7.5% w/w PHC loss (see TGA profile of pure PHC). In the second step (260-554°C) HYBD loosed a further 16% weight, corresponding to a 7.5% w/w PHC loss and to a 8.5% w/w CRV loss (calculated as difference). Finally the increase in temperature from 505° to 708°C produced a HYBD % weight loss equal to 5% w/w, related to a CRV loss of 2% w/w. Total % CRV loss from HYBD was about 20%, corresponding to the total % CRV loaded. The successful loading of CRV on PHC was confirmed by UV analysis of the supernatant obtained after CRV extraction in hexane from HYBD. The supernatant showed a maximum absorption peak at 275 nm. A CRV-hexane solution, subjected to UV spectrophotometer analysis, showed a maximum absorption peak at 275 nm, which is very close to the wavelength reported by Tunç and Duman (λ_{max} in n-hexane~273 nm) (Tunç and Duman, 2011).The amount of loaded CRV in 2 g of HYBD was 0.43 ± 0.02 g, corresponding to 21 ± 1 % w/w.

Figure 2B reports TGA curves of HYBD obtained at time 0 and after storage for 1 month at 20°C in dessicator. Storage conditions did not produce any change in % weight *vs* temperature profile, indicating that in such conditions HYBD was stable: no CVR was lost during storage.

These results indicate that PHC was able to reduce CRV volatility and that HYBD is a stable composite at temperatures lower than 80°C.

3.2 *In vitro* assessment of cytocompatibility, antioxidant and antimicrobial properties of CRV and HYBD

3.2.1 Cytocompatibility

In Figure 3 % viability values of fibroblasts treated with CRV and HYBD dissolved/dispersed in CM are reported. Different CRV concentrations, ranging from 10 to 100 μg/ml, were considered. The results indicate that CRV is cytocompatible at low concentrations (10 and 25 μg/ml), as pointed out by % viability values not statistically different from that of the reference (CM). At CRV

concentrations ≥ 50 μg/ml, a marked reduction in cell viability (76% at 50 μg/ml, and 0% at 100 μg/ml) was observed. These results confirm CVR cytotoxic effect reported by Coccimiglio et al. (2016). CVR produced a concentration-dependent decrease of cell number and total protein, accompanied by a degeneration of cell morphology. Another *in vitro* study pointed out CVR potent inhibitory effect of cell growth in A549 cell line (Koparal and Zeytinoglu, 2003). According to (Coccimiglio et al., 2016), the high CVR partition coefficient in octanol/water (3.64) is responsible for its deep partition in the cytoplasmatic membrane and a consequent alteration of cell permeability.

On the contrary, HYBD did not show any cytotoxic effect for all the concentrations investigated. These results pointed out that CRV loading in PHC is able to protect human fibroblasts against CRV cytotoxic effect. This is likely due to a slow release of CRV to cell membrane. On the basis of such hypothesis, it is necessary to verify if CVR loading in HYBD does not result in a decrease of CRV antioxidant properties.

3.2.2 Antioxidant properties

It is well known that the term oxidative stress expresses an increased formation of reactive oxygen species (ROS) and/or a decrease in their elimination. ROS are normal products of aerobic metabolism, an overproduction occurs under pathophysiological conditions. ROS damage cells, assaulting biological membrane lipids, nucleic acids, carbohydrates, and proteins (Jomova and Valko, 2011). Since H_2O_2 is produced *in vivo* by the spontaneous and/or enzymatic dismutation of the superoxide anion radical, it was used as a model of oxidative stress.

In Figure 4 % viability values of fibroblasts treated with H_2O_2 in presence and in absence of CRV pure or loaded in HYBD, are compared. Untreated cells, cultured in CM, were used as reference. A significant decrease of % viability is observed for fibroblasts treated with H_2O_2 in comparison with untreated cells, cultured in CM. This result pointed out the suitability of the experimental conditions (H_2O_2 concentration and contact time) to produce an oxidative damage. As expected, pretreatment of fibroblasts with CRV at nontoxic concentrations (10 and 25 μg/ml) resulted in a concentration-dependent protective effect against H_2O_2. Phenols such as CRV belong to the most active natural antioxidants found in the essential oils. According to some authors, *in vitro* antioxidant properties of oregano extracts, whose main component is CRV, are due to their free radical scavenger action (Ruberto and Baratta, 2000, Yanishlieva et al., 1999)

No significant differences were observed between CRV and HYBD, when tested at the same CRV concentration. It must be underlined that % viability values of fibroblasts treated with CRV, either pure or loaded in HYBD, were not significantly different from that observed for cells not treated

with the oxidative agent. It indicates CRV capability to protect human fibroblast from oxidative damage. The results obtained prove that CRV was able to protect human fibroblasts against oxidative stress and its loading in PHC did not affect such activity.

3.2.3 Antimicrobial properties

CRV antimicrobial properties are well-known. Lambert et al. (2001) attribute the antimicrobial activity of oregano essential oil and its active constituents (CVR and thymol) to interference with the pH gradient and membrane permeability. More recently, other authors have described that CVR may also be involved in inhibiting *E. coli* flagellin (Burt et al., 2004, 2007).

In Table 2 MIC and MBC values of pure CRV and HYBD are reported. Pure clay did not show antimicrobial activity at the concentrations considered. As expected, CRV showed antimicrobial properties. CRV loading into PHC produced a decrease of MIC and MBC values with respect to pure CRV. These results indicated a higher antimicrobial activity of CRV when loaded into clay. This effect could be attributed either to a lower evaporation (i.e. loss) of CRV when loaded into clay (see paragraph 3.1) and to a prolonged release of CVR from HYBD.

3.3 DoE assisted approach for film formulation

3.3.1 Full factorial design (FFD)

A full factorial design is useful to study the effect of each factor (X) and their interactions on the response variables (Y) (Dejagher and Vander Heyden, 2001). An analysis of variance was performed to test the statistical significance of the effects (positive or negative) of each factor and interaction on the various response parameters.

As for CRV loading into films, the supernatant (obtained after CVR extraction from film) gave a maximum peak of absorption at 275 nm, as observed for pure CRV and HYBD, confirming the presence of CRV into film. The loading amount was equal to 100 ± 9.8 %, with respect to the theoretical one. Such results indicate that the method employed for film preparation did not produce CRV loss.

Figure 5A reports the experimental results obtained for the film formulations, corresponding to the different experimental points of the FFD.

It can be observed that all films, except formulation 4 (characterized by the highest concentration of PVA and the lowest concentrations of PVP and CS) and formulation 5 (prepared with the highest PVP and CS concentrations and the lowest PVA concentration), were characterized by high elongation values. High % elongation indicates a high film deformability/flexibility, that is a high capability to deform under stress without breaking.

As for tensile stress, all the films maintained integrity when handled for mounting on the tensile apparatus. Stresses applied during such an assembly are reasonably greater than those involved during *in vivo* administration. Therefore, every film is likely to possess a mechanical resistance adequate to their use, which involves a mild manipulation. Anyway, formulations characterized by the lowest CS concentrations showed the highest strength values.

All the films prepared, with the exception of formulations 4 and 8, were able to absorb a buffer amount higher than their dry weight. Formulations 4 and 8 showed the lowest value of gel durability. Such formulations were characterized by low levels of both PVP and CS. The results demonstrate that such polymers were responsible for a slow and high hydration, corresponding to a slow erosion/dissolution and, consequently, to a high gel durability.

In Table 3, the estimated effects on each response variable and the corresponding P-values, calculated from Anova, for each factor and their interactions, are reported.

It can be observed that PVA and CS had a significant effect on % elongation, in particular an increase in PVA concentration caused an increase in such parameter; on the contrary, an increase in CS concentration determined a decrease of film elongation. Such response variable was not significantly affected by PVP concentration. All interactions between factors determined a significant effect on % elongation (see supplementary material). As for PVA-PVP interaction, when the lowest PVA level is considered, an increase in PVP concentration would determine a decrease of % elongation, while for the highest PVA level an increase in PVP concentration should produce an increase in film deformability. Conversely, for both PVA levels, an increase in CS concentration was expected to cause a decrease of % elongation value. As for PVP-CS interaction, the highest % elongation value was estimated for low levels of both PVP and CS.

As for tensile stress, PVP and CS had a significant negative effect, meaning that an increase in PVP or CS concentrations would produce a decrease of such parameter (Table 3), that is a weakening of film structure. These results are in agreement with that reported in literature. In particular, Hasan et al. (2017) observed a decrease in mechanical properties of films based on CS and PVP on increasing PVP concentration. Yeh et al. (2007) explained similar results with the rigid and fragile nature of PVP.

As for PVA-PVP and PVA-CS interactions, the highest tensile strength values were expected for the highest PVA level associated with the lowest PVP or CS levels (see supplementary material).

The results obtained indicate that between the two film forming polymers, PVA plays the main positive role on film mechanical properties. On the contrary, CS is responsible for film stiffening.

These results are in agreement with that recently observed by Malippedi et al. (2017). They prepared transdermal films by dissolving PVP and PVA in distilled water and employing glycerol as plasticizer agent. They observed an increase in tensile strength on increasing PVA concentration. Also Kim et al. (2015) prepared film based on PVP/PVA blends. They observed that films prepared at 4/10 and 6/8 w/w ratio produced weaker hardness compared to that with only PVA.

Both PVP and CS concentrations would positively affect film capacity to absorb a buffer mimicking wound exudate. Such polymers were expected to cause a slow and high film hydration.

The effect of PVP level was more pronounced for the highest CS concentration (see supplementary material). When PVP level was fixed at -1, an increase in CS concentration caused a marked decrease of PBS amount absorbed; on the contrary, in the presence of the highest PVP concentration, an increase in CS concentration determined a little decrease of such parameter. These results are in agreement with PVP high hydrophilicity (Hasan et al., 2017) and the poor CS solubility at neutral pH (Muzzarelli, 2009) .

PVP and CS concentrations also influence gel durability, that is gel capability to remain for a prolonged time at the wound site. In particular, an increase in PVP or CS concentrations would produce an increase in such parameter. PVP-CS interactions showed a significant effect.

This is due to the formation of hydrogen bonds between PVP and CS, involving OH of PVP and OH or NH_2 of CS (Hassan etal., 2017; Yeh et al., 2006).

3.3.2 Central composite design (CCD)

In Figure 5B the experimental results of the additional points investigated to expand FFD to CCD are reported.

Table 4 shows the estimated effects on each response variable and the corresponding P-values, calculated from Anova, for each factor and their interactions.

The expansion of FFD to CCD shows that no polymer concentration would individually affect film elongation. On the contrary, significant effects were determined for interactions, in particular a synergic effect for PVA-PVP and PVA-CS interactions and an antagonist one for PVP-CS interaction (see supplementary material). As for PVA-PVP and PVA-CS interactions, for low PVP or CS concentrations, an increase in PVA concentration would cause a decrease of % elongation; on the contrary, when PVP or CS level was fixed at + 1 an increase in PVA concentration would produce an increase in such parameter. As for PVP-CS interaction, the highest % elongation value was expected for the highest PVP and CS concentrations.

As for tensile stress, the extension of FFD to CCD evidenced a significant effect only for CS. No polymer interaction had a significant effect on such parameter.

As for PBS amount absorbed, the extension of FFD to CCD did not cause changes of the effects of each factor and their interactions, with the exception of PVP concentration, that did not significantly influence film hydration properties.

Also for gel durability no difference was determined by the extension of FFD to CCD.

Based on the results of the statistical analysis (Anova), an equation of the fitted model for each response variable was obtained. In particular, for each response variable, all the factors and/or their interactions that did not significantly affect the response parameter considered were excluded from the general polynomial regression equation. These models were graphically interpreted by drawing 2D contour plots, that represent the responses as functions of the levels of two factors, and 3D response surface plots, that show the responses in three dimensions. (Dejaegher and Vander Heyden, 2011).

The results of the statistical analysis (Anova) evidenced that, among the factors considered, PVA was the less influent on the response variables. For such reason, it was decided to keep the PVA level constant for the optimization procedure. To choose PVA concentration, the maximum value of each response variable predicted by the simplified fit models for each PVA level, was considered (Table 5).

Among PVA levels, only + 1.73 was estimated to produce films characterized by % elongation lower than 100%. High mechanical resistance, hydration propensity and gel durability were predicted for +1, 0 and -1 levels. Among these, the lowest PVA level (-1) was chosen for the continuation of the work.

In Figure 6 A, B, C, D, bi- and tri-dimensional plots drawn according to the simplified fit model for each response variable are reported.

The model predicted that the highest value of percent elongation is obtained for PVP and CS concentrations ranging, respectively, into the intervals -0.80 (2.2% w/w)/ +1.73 (4.73% w/w) and –0.67 (0.19% w/w) / +1.73 (0.634% w/w) (Figure 6A).

As for tensile strength (Figure 6B), counters plots evidenced the best performance for films characterized by low CS concentration (≤ 0.17% w/w), independently of PVP concentration.

As shown in Figure 6C the model predicted that film formulations, prepared with PVP and CS concentrations ranging, respectively, into the intervals 2.01% w/w (-0.99)/3.93% w/w (+0.93) and 0.27% w/w (-0.25)/0.59% w/w (+1.51), were characterized by high capability to absorb PBS, mimicking wound exudate.

The model describing the gel durability response predicted the highest value of such parameter for a PVP concentration between 1.46% w/w (-1.54) and 3.37% w/w (+0.37) and a high CS concentration (≥ 0.431% w/w; +0.62) (Figure 6D).

In general optimal performances do not correspond to a single point but a region of the experimental domain. For this reason, the individual 2D contour plots were superimposed in order to identify the optimal region of domain, capable of satisfying the following constraints: percent elongation ≥ 80%; 3 N/mm^2 ≥ tensile strength ≥ 2.4 N/mm^2 ; PBS absorbed/unit weight ≥ 1.0 g/g; gel durability ≥ 0.6 g. Such constrains characterized optimal film performance. In fact, a high film flexibility is advisable, since an easy deformation allows a comfortable and simple administration; a suitable mechanical resistance (tensile strength) is required to maintain film integrity during packaging; a good capability to absorb the excess wound exudate and a prolonged film permanence on the wound site are features useful for wound healing. In case of exudative chronic wounds, solid dressings are preferred to liquid/semisolid preparations because the formers are able to absorb the excess exudate, rich in metalloproteinases, and to maintain wetting conditions optimal for healing (Boateng and Catanzano, 2015).

The formulation of optimized composition, chosen inside the region evidenced in Figure 7, was: PVA 11.3% w/w - PVP 2.4% w/w – CS 0.46% w/w – Ser 0.8 % w/w – PHC 2% w/w – Gly 10% w/w.

Table 6 reports the predicted and experimental values obtained for the various properties of the film of optimized composition. It can be observed that the experimental values were comparable to the fitted ones at 95% confidence level. This confirms the prediction power of the regression models.

3.4 Characterization of optimized formulation (opFILM)

3.4.1 Rheological properties

In Figure 8 loss tangent (tan delta) profile as a function of frequency of hydrated opFILM film is reported. It can be observed that tan delta values, independently of the frequency, were lower than 1, indicating that the gel formed after hydration was characterized by a prevalence of elastic (G′ modulus) on viscous (G″ modulus) properties (Rossi et al, 2007). High elastic properties are advisable since they are related to gel protective action towards lesion area.

3.4.2 *in vitro* release properties

In Figure 9 % CRV release profiles of opFILM and HYBD are reported. Significant ($p<0.05$) differences are observed only at 4 and 8 hours: film was characterized by lower values with respect to HYBD. This result is conceivably due to the formation of a viscoelastic gel that slowed down

CRV diffusion. The superimposition of the released profiles observed after 8h can be explained by gel dissolution: CRV release was only controlled by HYBD.

4 CONCLUSIONS

CRV loading into PHC results in maintenance of CRV antioxidant properties, improvement of its cytotoxicity towards human fibroblast and increase in antimicrobial properties. These results are due to PHC protection against CRV evaporation. Thanks to DoE approach, film characterized by optimal technological properties was determined. In particular, exploiting PVA film forming properties and CS and PVP interaction, film characterized by optimal mechanical and hydration properties was obtained. It was able upon hydration to form a viscoelastic gel capable of protecting lesion area and modulating CRV release. The overall results indicate that the optimized formulation is a promising candidate for the treatment of chronic skin ulcers. The following step of the research will focus on formulation performance on in vivo animal model, set up by the research group (Tenci et al., 2016, 2017), in comparison with commercial dressings.

Acknowledgements

This study was partially supported by the Spanish project CGL2016-80833-R of the Ministerio de Economía, Industria y Competitividad (MEIC).

5. REFERENCES

Abshar, H., Waibhaw, G., Tiwari, S., Dharmalingam, K., Shukla, I., Pandey, L. M., 2017. Fabrication and characterization of chitosan, polyvinylpyrrolidone, and cellulose nanowhiskers nanocomposite films for wound healing drug delivery application. DOI: 10.1002/jbm.a.3609

Bakkali, F., Averbeck, S., Averbeck, D., Idaomar, M., 2008. Biological effects of essential oils ‐ A review. Food Chem. Toxicol. 46, 446‐475.

Ben Arfa, A., Combes, S., Preziosi-Belloy, L., Gontard, N., Chalier, P., 2006. Antimicrobial activity of carvacrol related to its chemical structure. Lett. Appl. Microbiol. 43, 149–154.

Boateng, J., Catanzano, O., 2015. Advanced therapeutic dressings for effective wound healing-A review. J. Pharm. Sci. 104, 3653–3680.

Boateng, J.S., Matthews, K.H., Stevens, H.N., Eccleston, G.M., 2008.Wound healing dressings and drug delivery systems: a review. J. Pharm. Sci. 97, 2892–2923.

Burt, S., 2004. Essential oils: their antibacterial properties and potential applications in foods - a review. Int. J. Food. Microbiol. 94, 223–253

Burt S., van der Zee, R., Koets, A. P., de Graaff, A. M., van Knapen, F., Gaastra, W., Haagsman, H. P., Veldhuizen, E.J.A. 2007. Carvacrol induces heat shock protein 60 and inhibits synthesis of flagellin in Escherichia coli O157:H7. Applied and Environmental Microbiology 73, 4484–4490.

Clinical and Laboratory Standards Institute, Methods for Determining Bactericidal Activity of Antimicrobial Agents: Approved Guideline M26-A, Clinical and Laboratory Standards Institute, Wayne, PA, USA, 1999

Clinical and Laboratory Standards Institute, Methods for Determining Bactericidal Activity of Antimicrobial Agents: Approved Guideline M26-A, 1999. Clinical and Laboratory Standards Institute, Wayne, PA, USA,

Clinical and Laboratory Standards Institute, Methods for Dilution Antimicrobial Susceptibility Tests for Bacteria That Grow Aerobically-Eighth Edition: Approved Standard M7-A8, 2009. Clinical and Laboratory Standards Institute, Wayne, PA, USA.

Campos-Requena, V.H., Rivas, B.L., Pérez, M.A., Figueroa, C.R., Sanfuentes, E.A., 2015. The synergistic antimicrobial effect of carvacrol and thymol in clay/polymer nanocomposite films over strawberry gray mold. LWT-Food Sci. Technol. 64, 390–396.

Coccimiglio, J., Alipour, M., Jiang, Z.-H., Gottardo, C., Suntres, Z.. 2016. Antioxidant, antibacterial, and cytotoxic activities of the ethanolic *Origanum vulgare* extract and its major constituents. Oxidative Medicine and Cellular Longevity, Article ID 1404505.

Comolli, N., Donaldson, O., Grantier, N., Zhukareva, V., Tom, V.J., 2012. Polyvinyl alcohol-polyvinyl pyrrolidone thin films provide local short-term release of anti-inflammatory agents post spinal cord injury. J. Biomed. Mater. Res. B. Appl. Biomater. 100, 1867–1873.

Contardi, M., Heredia-Guerrero, J.A., Perotto, G., Valentini, P., Pompa, P. P., Spano, R., Goldoni, L., Bertorelli, R., Athanassiou, A., Bayer, I. S., 2017. Transparent ciprofloxacin-povidone antibiotic films and nanofiber mats as potential skin and wound care dressings. European Journal of Pharmaceutical Sciences 104, 133-144.

Dejagher, B., Vander Heyden, Y., 2009. The use of experimental design in separation science. Acta Chromatogr. 21, 161- 201.

Dejagher, B., Vander Heyden, Y., 2011. Experimental designs and their recent advances in set-up, data interpretation, and analytical applications. J. Pharm. Biomed. Anal. 56, 141-158.

Edris, A,E., 2007. Pharmaceutical and therapeutic potentials of essential oils and their individual volatile constituents: a review. Phytother. Res. 21, 308–323.

Efrati, R., Natan, M., Pelah, A., Haberer, A., Banin, E., Dotan, A., Ophir, A., 2014. The combined effect of additives and processing on the thermal stability and controlled release of essential oils in antimicrobial films. J. Appl. Polym. Sci. 131, 40564-40574.

El-Malah Y., Nazzal S., 2008. Novel use of Eudragit® NE 30D/Eudragit® L 30D-55 blends as functional coating materials in time-delayed drug release applications. Int. J. Pharm. 357, 219–227.

Gorrasi, G., 2015. Dispersion of halloysite loaded with natural antimicrobials into pectins: characterization and controlled release analysis. Carbohyd. Polym. 127, 47–53.

Guo, R., Du, X., Zhang, R., Deng, L., Dong, A., Zhang, J., 2011. Bioadhesive film formed from a novel organic-inorganic hybrid gel for transdermal drug delivery system. Eur. J. Pharm. Biopharm. 79, 574–583.

Higueras, L., López-Carballo, G., Cerisuelo, J.P., Gavara, R., Hernández-Muñoz, P., 2013. Preparation and characterization of chitosan/HP-β-cyclodextrins composites with high sorption capacity for carvacrol. Carbohyd. Polym. 97, 262– 268.

Kim, D.W., Kim, K. S., Seo, Y. G., Lee B.-J., Park, Y. J., Yound,Y. S., Kim, J. O. , Yong, C. S., Jin, S. G., Choi, H.-G., 2015. Novel sodium fusidate-loaded film-forming hydrogel with easy application and excellent wound healing. Int. J. Pharm. 495, 67- 74

Koparal, A. T., and Zeytinoglu, M.. 2003. Effects of carvacrol on a human non-small cell lung cancer (NSCLC) cell line, A549. Cytotechnology 43, 149–154.

Jomova, K. and Valko, M., 2011. Advances in metal-induced oxidative stress and human disease, Toxicology 283, 65– 87.

Lambert, R. J. W., Skandamis, P. N., Coote, P. J., Nychas G.-J. E., 2001. A study of the minimum inhibitory concentration and mode of action of oregano essential oil, thymol and carvacrol. Journal of Applied Microbiology 91, 453–462.

Li, J., Zivanovic, S., Davidson, P.M., Kit, K., 2010. Characterization and comparison of chitosan/PVP and chitosan/PEO blend films. Carbohyd. Polym. 79, 786–791.

López-Galindo, A., Viseras, C., Cerezo, P., 2007. Compositional, technical and safety specifications of clays to be used as pharmaceutical and cosmetic products. Appl. Clay Sci., 36: 51–63.

Malipeddi, V. R., Awasthi, R., Dal Molim Ghisleni D., de Souza Braga, M., Satiko Kikuchi, I., Andreoli Pinto,T., Dua, K., 2017. Preparation and characterization of metoprolol tartrate containing matrix type transdermal drug delivery system. Drug Deliv. and Transl. Res. 7, 66–76.

Miguel, M.G., 2010. Antioxidant and anti-inflammatory activities of essential oils: a short review. Molecules 15, 9252-9287.

Mori, M., Rossi, S., Bonferoni, M.C., Ferrari, F., Sandri, G., Riva, F., Del Fante, C., Perotti, C., Caramella, C., 2014. Calcium alginate particles for the combined delivery of platelet lysate and vancomycin hydrochloride in chronic skin ulcers. Int. J. Pharm. 461, 505–513.

Mori, M., Rossi, S., Ferrari, F., Bonferoni, M.C., Sandri, G., Chlapanidas, T., Torre, M.L., Caramella, C., 2016. Sponge-like dressings based on the association of chitosan and sericin for the treatment of chronic skin ulcers. I. Design of experiments-assisted development. J. Pharm. Sci. 105, 1180-1187.

Muzzarelli, R.A.A., 2009. Chitins and chitosans for the repair of wounded skin nerve, cartilage and bone. Carbohydr. Polym. 76, 167–182.

Paula, A.J. R., 1, Azevedo, A.M., Aires-Barros M. R., 2007. Application of central composite design to the optimisation of aqueous two-phase extraction of human antibodies.Journal of Chromatography A 1141, 50–60.

Peng, Y., Zhang, H., Liu, R., Mine, Y., McCallum, J., Kirby, C., Tsao, R., 2016. Antioxidant and anti-inflammatory activities of pyranoanthocyanins and other polyphenols from staghorn sumac (*Rhus hirta L.*) in Caco-2 cell models. .J Funct. Foods 20, 39–147.

Rossi, S., Marciello, M., Bonferoni, M.C., Ferrari, F., Sandri, G., Caramella, C., Dacarro, C., Grisoli, P., 2010. Thermally sensitive gels based on chitosan derivatives for the treatment of oral mucositis. Eur. J. Pharm. Biopharm. 74, 248–254.

Rossi, S., Marciello, M., Sandri, G., Ferrari, F., Bonferoni, M.C., Papetti, A., Caramella, C., Dacarro, C., Grisoli P., 2007. Wound dressings based on chitosans and hyaluronic acid for the release of chlorhexidine diacetate in skin ulcer therapy. Pharmaceutical development and technology 12, 415-422.

Rossi, S., Faccendini, A., Bonferoni, M.C., Ferrari, F., Sandri, G., Del Fante, C., Perotti, C., Caramella, C., 2013. Sponge-like dressings based on biopolymers for the delivery of platelet lysate to skin chronic wounds. Int. J. Pharm. 440, 207–215.

Rossi, S., Ferrari, F., Sandri, G., Bonferoni, M.C., Del Fante, C., Perotti, C., Caramella, C., 2015. Wound healing: biopolymers and hemoderivatives, 1st ed. In: Mishra, M. (Ed.), Encyclopedia of Biomedical Polymers and Polymeric Biomaterials, vol. 11. Taylor & Francis, New York, pp. 8280–8298.

Ruberto, G. and Baratta, M. T., 2000. Antioxidant activity of selected essential oil components in two lipid model systems. Food Chemistry 69, 167–174.

Safaei-Ghomi, J., Ebrahimabadi, A.H., Djafari-Bidgoli, Z., Batooli, H., 2009. GC/MS analysis and *in vitro* antioxidant activity of essential oil and methanol extracts of *Thymus caramanicus* Jalas and its main constituent carvacrol. Food. Chem. 115, 1524–1528.

Sanchez-Espejo, R, Aguzzi, C, Salcedo, I, Cerezo, P., Viseras, C., 2014. Clays in complementary and alternative medicine. Materials Technology 29, B78-B81.

Seabra, A.B., De Oliveira, M.G., 2004. Poly(vinyl alcohol) and poly(vinyl pyrrolidone) blended films for local nitric oxide release. Biomaterials 25, 3773–3782.

Shemesh, R., Krepker, M., Natan, M., Danin-Poleg, Y., Banin, E., Kashi, Y., Nitzan, N., Vaxmanb, A., Segal, E., 2015. Novel LDPE/halloysite nanotube films with sustained carvacrol release for broad-spectrum antimicrobial activity. RSC Adv. 5, 87108 –87117.

Singh, B., Pal, L., 2011. Radiation crosslinking polymerisation of sterculia polysaccharide-PVA-PVP for making hydrogel wound dressings. Int. J. Biol. Macromol. 48, 501–510.

Sreedharan N. R., Sujith N. 2015. Permeation Studies of Captopril Transdermal Films Through Human Cadaver Skin. Current drug delivery 12(5), 517-23.

Tenci, M., Rossi, S., Bonferoni, M.C., Sandri, G., Boselli, C., Di Lorenzo, A., Daglia, M., Icaro Cornaglia, A., Gioglio, L., Perotti, C., Caramella, C., Ferrari, F., 2016a. Pectin/chitosan particles for the delivery of platelet lysate and manuka honey in chronic skin ulcers. Int. J. Pharm. 509, 59-70.

Tenci, M., Rossi, S., Bonferoni, M.C., Sandri, G., Mentori, I., Boselli, C., Icaro Cornaglia, A., Daglia, M., Marchese, A., Caramella, C., Ferrari, F., 2017. Application of DoE approach in the development of mini-capsules, based on biopolymers and Manuka honey polar fraction, as powder formulation for the treatment of skin ulcers, Int. J. Pharm. 1-2, 266- 277.

Tunç, S., Duman, O., 2011. Preparation of active antimicrobial methyl cellulose/carvacrol/ montmorillonite nanocomposite films and investigation of carvacrol release. LWT - Food Sci. Technol. 44, 465-472.

Vicentini, D.S., Smania, A., Laranjeira, M.C.M., 2010. Chitosan/poly(vinyl alcohol) films containing ZnO nanoparticles and plasticizers. Mat. Sci. Eng. C. 30, 503-508.

Viseras, C, Aguzzi, C, Cerezo, P, Bedmar, MC., 2008. Biopolymer-clay nanocomposites for controlled drug delivery. Materials Science and Technology 24, 1020-1026.

Viseras, C., Cerezo, P., Sanchez, R., Salcedo, I., Aguzzi, C., 2010. Current challenges in clay minerals for drug delivery. Appl. Clay Sci. 40, 291–295.

Yanishlieva, N. V., Marinova, E. M., Gordon, M. H., Raneva ,V.G., 1999. Antioxidant activity and mechanism of action of thymol and carvacrol in two lipid systems. Food Chemistry 64, 59–66.

Yeh, J.T., Chen, C.L., Huang, K., Nien, Y., Chen, J., Huang, P., 2006. Synthesis, characterization, and application of PVP/chitosan blended polymers.J Appl Polym Sci 101, 885–891.

LEGENDS:

Figure 1: % CRV loading capacity (%LC) of the three different CRV/clay hybrids prepared: A) by adsorption in saturated atmosphere technique at different temperatures (20, 40, 60, 80, 120°C) for 48 h; B) shear mixing technique (mean values n= 3; CV% < 10%).

Figure 2: Comparison of % weight *vs* temperature profiles of: A) PHC, CRV, and HYBD; B) HYBD at time 0 and after storage for 1 month in dessicator, at 20°C.

Figure 3: Comparison of % viability values of CRV (10 - 100 µg/ml) and HYBD dissolved/dispersed in CM. HYBD amounts corresponding to 10 -100 µg/ml CVR concentrations were considered. CM was used as reference (mean values ± s.e; n=8). Anova one way - MRT ($p<0.05$): a *vs* d/e; b *vs* d/e; c *vs* d/e; d *vs* e/d′; e *vs* e′; c′ *vs* e′.

Figure 4: % cell viability of fibroblasts subjected to oxidative damage (0.5 mM H_2O_2 for 6h), treated or untreated with CRV (10 and 25 µg/ml), either pure or loaded in HYBD. HYBD amounts corresponding to 10 and 25 µg/ml CVR concentrations were considered. Untreated cells, cultured in CM, were used as reference (mean values ± s.e; n=8). Anova one way - MRT ($p<0.05$): a *vs* b; b *vs* c/d/c´/d´; c *vs* d/d´; c´ *vs* d´.

Figure 5: Response variables of the films of FFD (A) and CCD (B) (mean values ± s.d.; n = 3). Anova one way - multiple range test ($p<0,05$)

a vs d/e/g/i/l/m; b vs d/e/g/i/l/m; c vs d/e/g/i/l/m; d vs f/g/h/i/l/m/n/o/p/q; e vs f/g/h/i/l/m/n/o/p/q; f vs g/I/i/m; g vs h/i/n/o/p/q; h vs i/l/m; i vs l/n/o/p/q; l vs m/n/o/p/q; m vs n/o/p/q; a′ vs b′/c′/d′/e′/f′/g′/h′/i′/l′/m′/n′/o′/p′/q′; b′ vs c′/d′/e′/g′/i′/l′/m′/n′/p′/q′; c′ vs d′/f′/h′/i′/l′/m′/n′/o′/p′/q′; d′ vs e′/f′/g′/n′/o′; e′ vs f′/h′/i′/l′/m′/n′/o′/p′/q′; f′ vs g′/i′/l′/m′/n′/p′/q′; g′ vs h′/ i′/l′/m′/n′/o′/p′/q′; h′ vs i′/n′/q′; i′ vs l′/n′/o′/p′/q′; l′ vs n′; m′ vs n′/o′; n′ vs o′/p′/q′; o′ vs p′/q′; a″ vs d″/i″/p″; b″ vs d″/f″/h″/i″/l″/m″/n″/p″; c″ vs d″/h″/I″/m″/p″; d″ vs e″/f″/g″/o″/q″; e″ vs h″/i″/m″/p″; f″ vs p″/q″; g″ vs h″/i″/l″/m″/n″/p″; h″ vs o″/p″/q″; i″ vs o″/p″/q″; l″ vs o″/p″/q″; m″ vs o″/p″/q″; n″ vs o″/p″/q″; o″ vs p″; p″ vs q″; a‴ vs d‴/f‴/h‴/i‴/n‴/p‴; b‴ vs d‴/f‴/h‴/i‴/n‴/p‴; c‴ vs d‴/ h‴/i‴/o‴/p‴; d‴ vs e‴/f‴/g‴/h‴/ l‴/m‴/o‴/p‴; e‴ vs h‴/i‴/n‴/p‴; f‴ vs i‴/n‴/p‴; g‴ vs h‴/n‴/p‴; h‴ vs i‴/l‴/m‴/n‴/p‴; i‴ vs l‴/m‴/n‴/o‴/q‴; l″ vs o‴/q‴; m‴ vs o‴/p‴; n‴ vs o‴/p‴/q‴; o‴ vs p‴; p‴ vs q‴.

Figure 6: Contour plots (in bi- and tri- dimensional projections) drawn according to simplified polynomial model for each response variable of CCD.

Figure 7: Region of optimal film composition which satisfies all the constraints of the response variables.

Figure 8: Loss tangent (G″/G′) values as a function of frequency obtained for opFILM at a constant shear stress (50 Pa) (mean values ± s.d; n=3).

Figure 9: % CRV released as a function of time for opFILM and HYBD (mean values ± s.e.; n=3). T-test ($p<0.05$): a *vs* b/c/d/a′ ; b *vs* c/d/b′; c *vs* d;. a' *vs* b'/c'/d'; b' *vs* c'/d′; c' *vs* d′.

Table(s)

Table 1 - Experimental points of FFD and CCD.

	Experimental Points	PVA	PVP	CS
Full Factorial Design		+1	+1	+1
	2	+1	+1	-1
	3	+1	-1	+1
	4	+1	-1	-1
Central Composite Design	5	-1	+1	+1
	6	-1	+1	-1
	7	-1	-1	+1
	8	-1	-1	-1
	9	0	-1.73	0
	10	0	+1.73	0
	11	+1.73	0	0
	12	-1.73	0	0
	13	0	0	+1.73
	14	0	0	-1.73
	15	0	0	0

PVA: level -1 (12%); level +1 (14%); level -1.73 (11.27%); level +1.73 (14.73%); level 0 (13%).
PVP: level -1 (2%); level +1 (4%); level -1.73 (1.27%); level +1.73 (4.73%); level 0 (3%).
CS: level -1 (0.134%); level +1 (0.5%); level -1.73 (0%); level +1.73 (0.634%); level 0 (0.317%).

Table 2 - MIC (minimum inhibition concentration) and MBC (minimum bactericidal concentration) values of pure CRV and HYBD against *Escherichia coli* and *Staphylococcus aureus*. MIC and MBC are expressed as CRV concentration (mean values (s.d), n=3).

	MIC (mg/ml)		MBC (mg/ml)	
	E. coli ATCC: 10536	*S. aureus* ATCC: 6538	*E. coli* ATCC: 10536	*S. aureus* ATCC: 6538
CRV	1.26 (0.41)	0.65 (0.27)	2.75 (0.65)	2.75 (0.65)
HYBD	0.60 (0.18)	0.26 (0.04)	1.18 (0.26)	0.49 (0.22)

Table 3 -Estimated effects and their statistical significance (P-values) of each factor and their interactions on each response variable of FFD.

	% E (mm/mm)		**TS (N/mm^2)**		**gPBS/g**		**Gel durability (g)**	
	Estimated effect	*P-value*	*Estimated effect*	*P-value*	*Estimated effect*	*P-value*	*Estimated effect*	*P-value*
A: PVA	7.34667	0.0418	-0.102667	0.1689	-0.0285	0.7715	-0.00425	0.8935
B: PVP	2.42333	0.4775	-0.462833	0.0000	0.228667	0.0300	0.162083	0.0001
C: CS	-7.34667	0.0418	-1.19383	0.0000	0.259167	0.0157	0.156917	0.0001
AB	23.3583	0.0000	-0.2105	0.0090	0.197167	0.0570	0.108583	0.0029
AC	33.1283	0.0000	-0.332167	0.0002	-0.097	0.3292	0.00741667	0.8154
BC	-23.3583	0.0000	0.0193333	0.7900	-0.318833	0.0042	-0.11625	0.0017

* p-values lower than 0.05 correspond to a statistical significant effect.

Table 4 -Estimated effects and their statistical significance (P-values) of each factor and their interactions on each response variable of CCD.

	% E		**TS (N/mm^2)**		**gPBS/g**		**Gel amount (g)**	
	Estimated effect	*P-value**	*Estimated effect*	*P-value**	*Estimated effect*	*P-value**	*Estimated effect*	*P-value**
A: PVA	-3.43942	0.2935	-0.215376	0.2998	-0.0374002	0.6764	0.0181086	0.5219
B: PVP	6.28152	0.0598	-0.375657	0.0752	0.178422	0.0528	0.179139	0.0000
C: CS	-4.1981	0.2016	-0.837745	0.0003	0.408563	0.0001	0.222457	0.0000
AB	23.3583	0.0000	-0.2105	0.4419	0.197167	0.1028	0.108583	0.0060
AC	33.1283	0.0000	-0.332167	0.2281	-0.097	0.4150	0.00741667	0.8424
BC	-23.3583	0.0000	0.0193333	0.9434	-0.318833	0.0105	-0.11625	0.0035

* p-values lower than 0.05 correspond to a statistical significant effect.

Table 5 - Maximum estimated effects of each PVA level on the response variables

PVA level	**%E**	**TS (N/mm^2)**	**gPBS/g**	**Gel durability (g)**
-1.73	139.454	2.98	1.139	0.65
-1	131.45	3.22	1.458	0.73
0	117.97	3.22	1.578	0.73
+1	117.7	3.22	1.420	0.78
+1.73	80.8	2.98	1.074	0.68

Table 6 - Predicted and experimental values of the formulation of optimized composition (mean values ± ds; n=3)

Response	**Predicted values ($p<0.05$)**	**Experimental values**
%E (mm/mm)	87 ± 4.3	92 ± 11
TS (N/mm^2)	2.6 ± 0.13	2.7 ± 0.14
gPBS/g	1.44 ± 0.072	1.44 ± 0.080
Gel durability (g)	0.70 ± 0.035	0.703 ± 0.005

Figure(s)

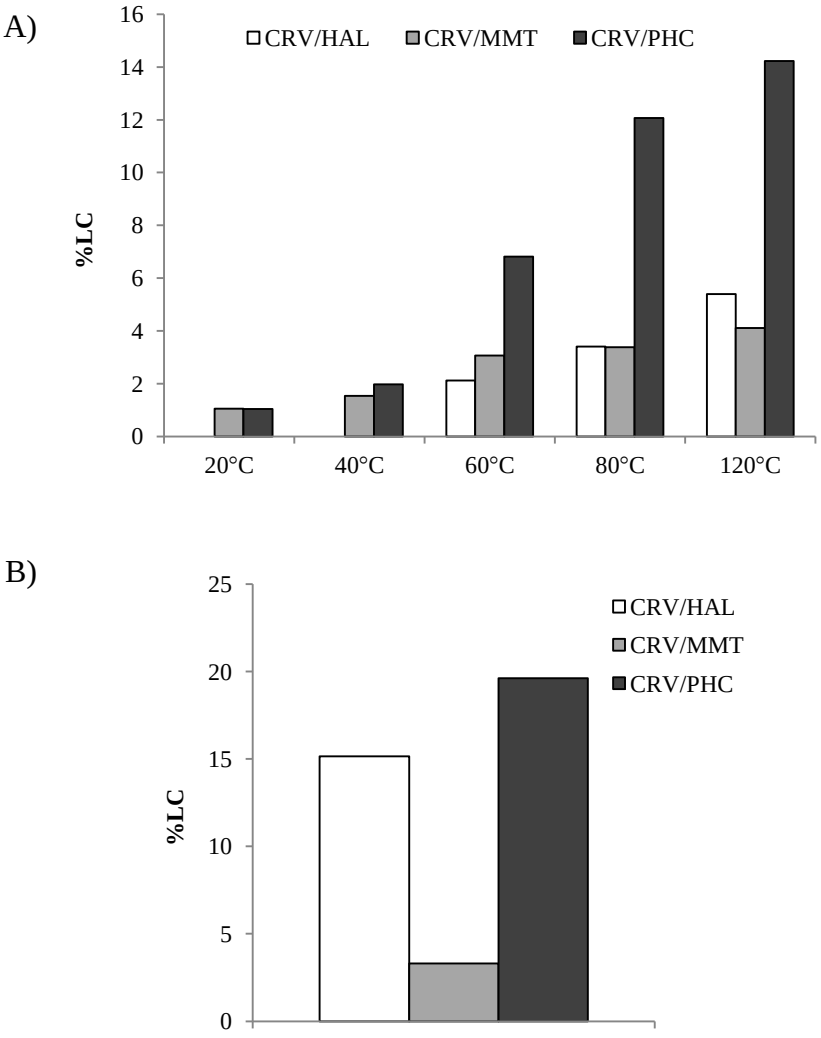

Figure 1

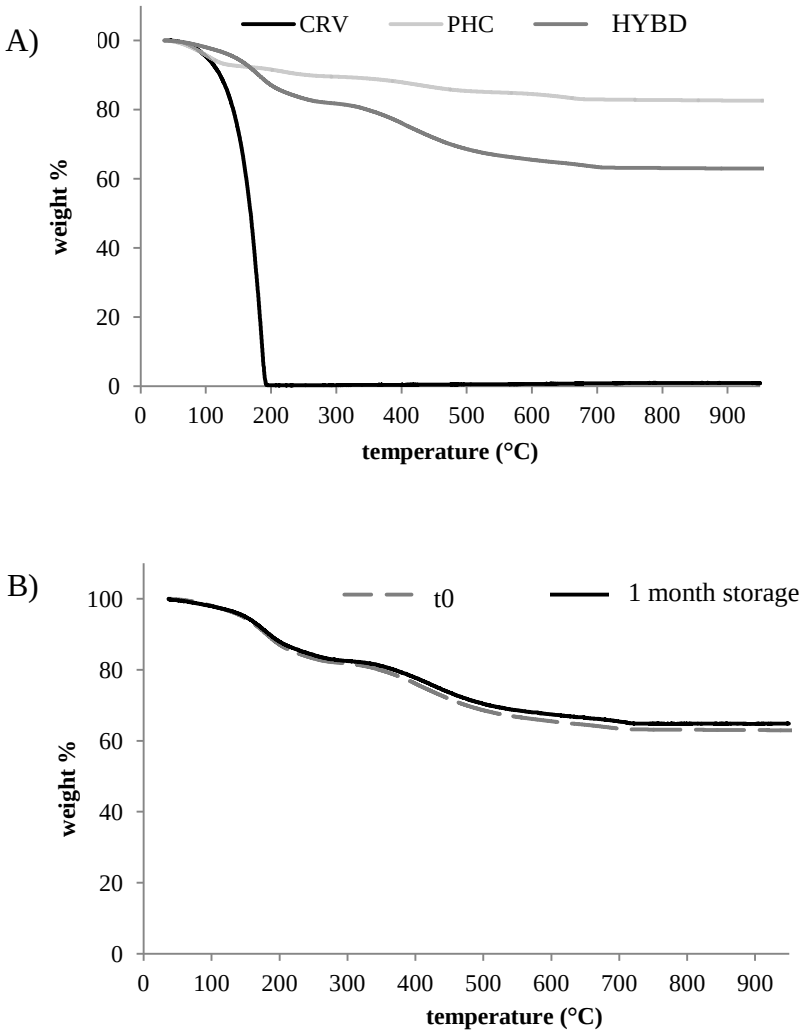
A)
CRV
PHC
HYBD
weight %
00
80
60
40
20
0
0
100
200
300
400
500
600
700
800
900
temperature (°C)
B)
t0
1 month storage
weight %
100
80
60
40
20
0
0
100
200
300
400
500
600
700
800
900
temperature (°C)

Figure 2

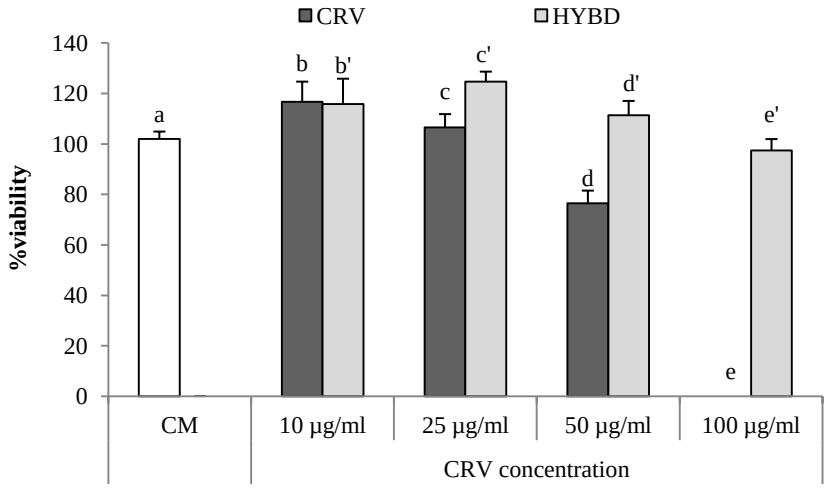

Figure 3

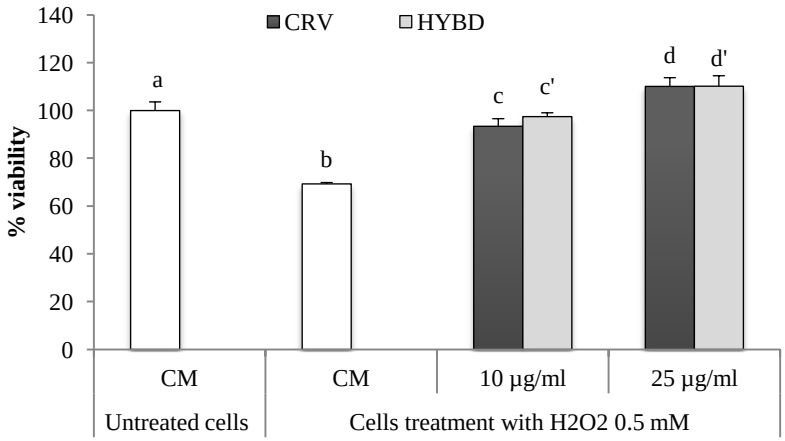

Figure 4

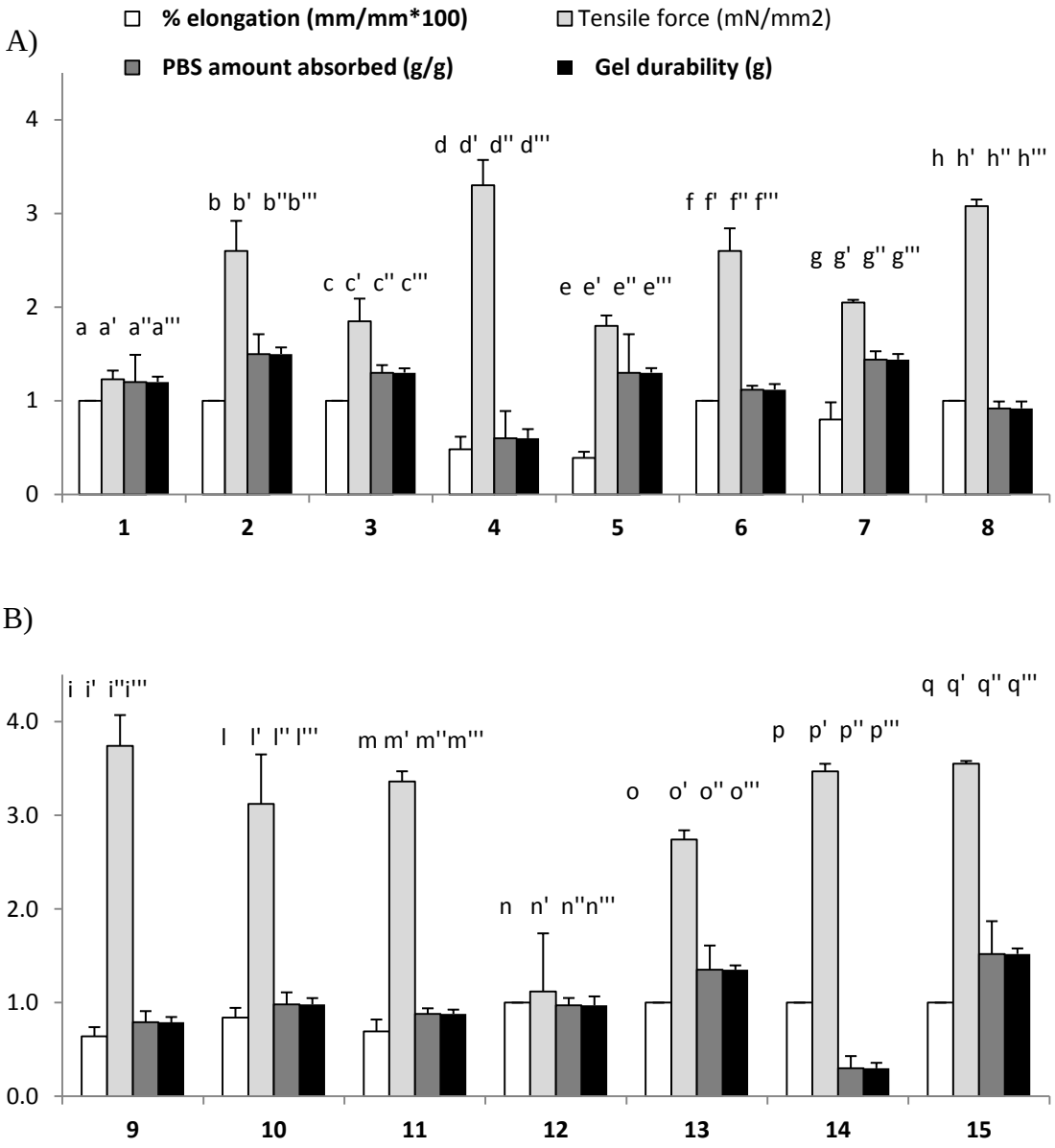
A)
% elongation (mm/mm*100)
Tensile force (mN/mm2)
PBS amount absorbed (g/g)
Gel durability (g)
4
3
2
1
0
a a' a''a'''
b b' b''b'''
c c' c'' c'''
d d' d'' d'''
e e' e'' e'''
f f' f'' f'''
g g' g'' g'''
h h' h'' h'''
1
2
3
4
5
6
7
8
B)
4.0
3.0
2.0
1.0
0.0
i i' i''i'''
l l' l'' l'''
m m' m''m'''
n n' n''n'''
o o' o'' o'''
p p' p'' p'''
q q' q'' q'''
9
10
11
12
13
14
15

Figure 5

A)

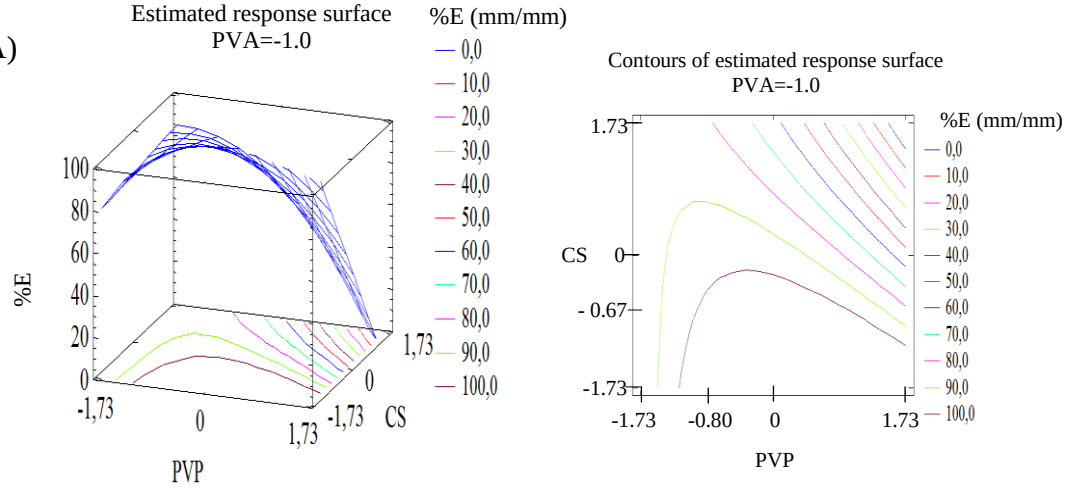
Estimated response surface
PVA=-1.0
%E (mm/mm)
0,0
10,0
20,0
30,0
40,0
50,0
60,0
70,0
80,0
90,0
100,0
%E
100
80
60
40
20
0
-1,73
0
1,73
PVP
CS
Contours of estimated response surface
PVA=-1.0
1.73
0
- 0.67
-1.73
-0.80
1.73
PVP
CS

B)

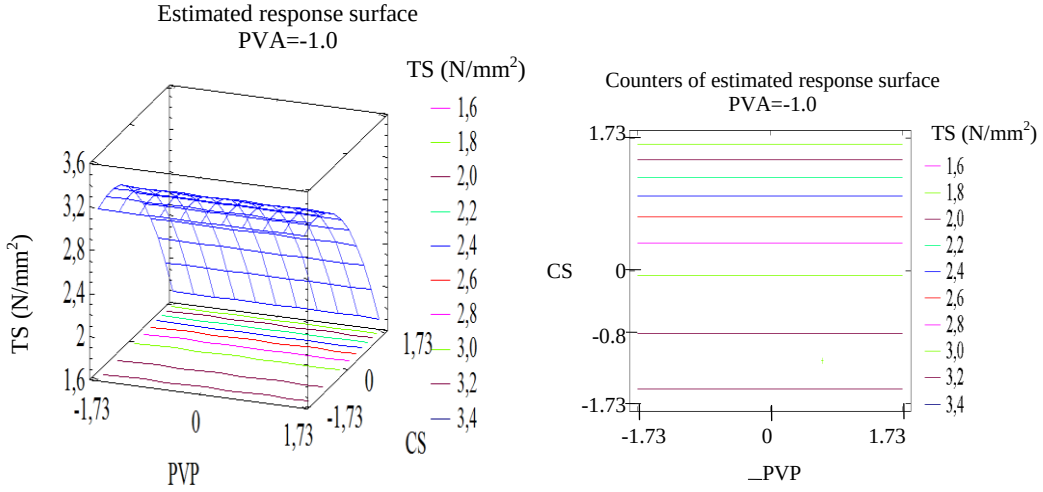
Estimated response surface
PVA=-1.0
TS (N/mm2)
1,6
1,8
2,0
2,2
2,4
2,6
2,8
3,0
3,2
3,4
TS (N/mm2)
3,6
3,2
2,8
2,4
2
1,6
PVP
CS
Counters of estimated response surface
PVA=-1.0
1.73
0
-0.8
-1.73
_PVP
CS

C)

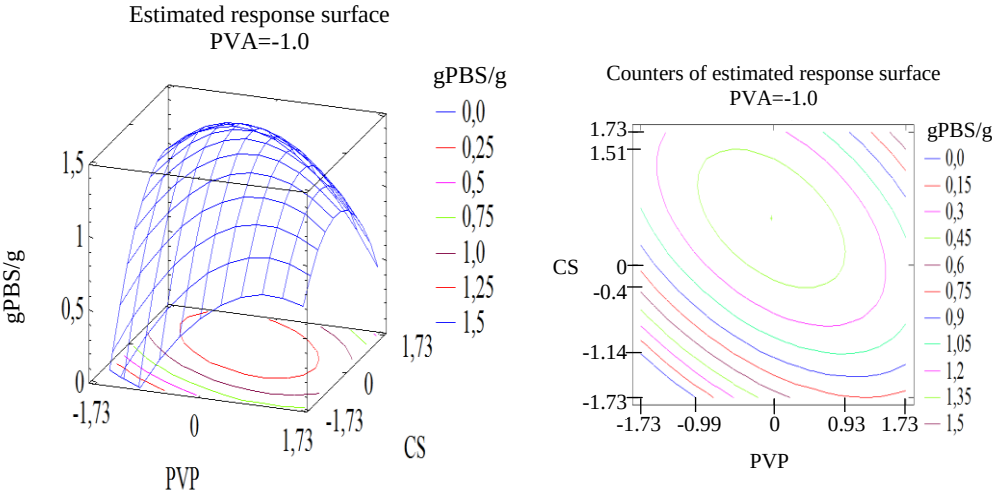
Estimated response surface
PVA=-1.0
gPBS/g
0,0
0,25
0,5
0,75
1,0
1,25
1,5
gPBS/g
1,5
1
0,5
0
PVP
CS
Counters of estimated response surface
PVA=-1.0
1.73
1.51
0
-0.4
-1.14
-1.73
-0.99
0.93
PVP
CS

D)

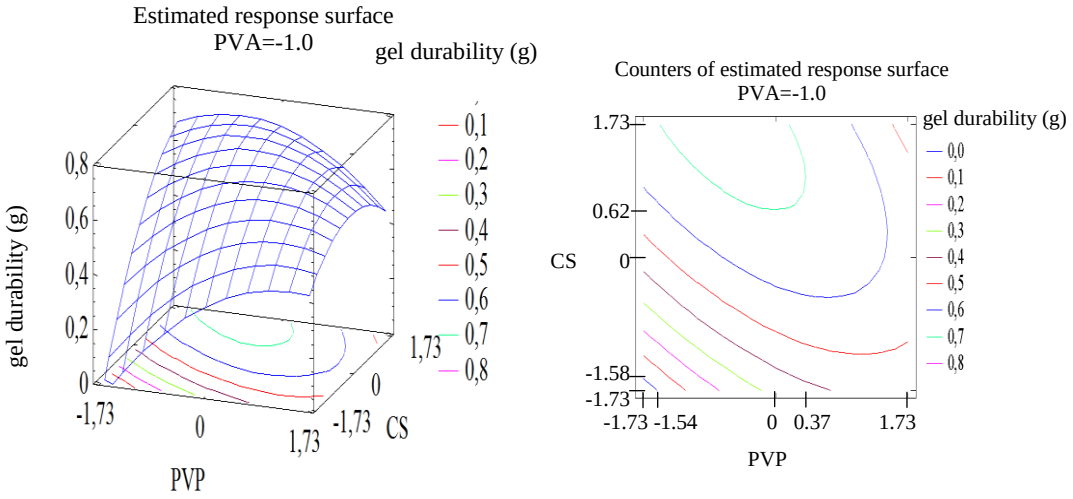

Figure 6

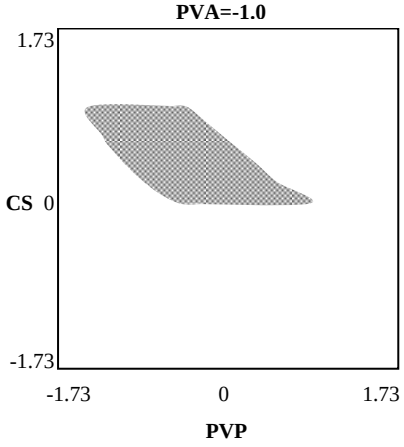

Figure 7

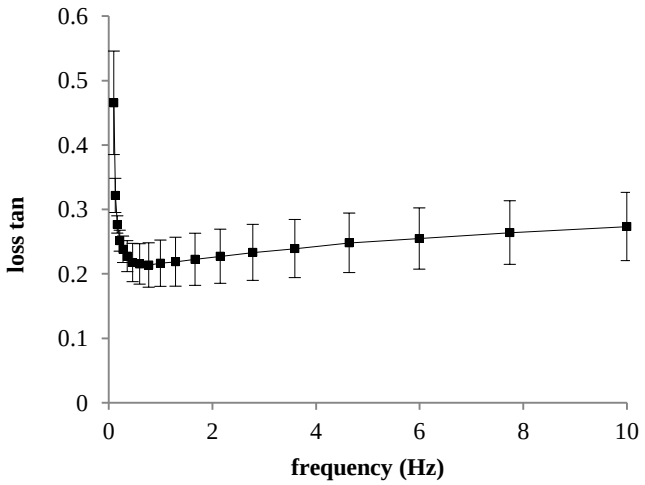

Figure 8

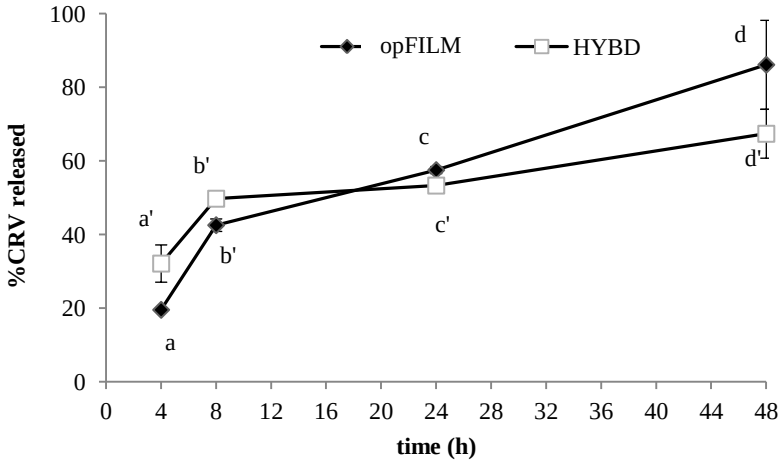

Figure 9

Supplementary Material

Click here to download Supplementary Material: Supplementary material.docx